Cancer Immunology, Immunotherapy (2021) 70:2235–2245
https://doi.org/10.1007/s00262-020-02753-y

ORIGINAL ARTICLE

LncRNA UCA1 attenuated the killing effect of cytotoxic CD8 + T cells on anaplastic thyroid carcinoma via miR-148a/PD-L1 pathway

Xiaoming Wang[1,2] · Yan Zhang[3] · Jian Zheng[1,2] · Cuixian Yao[1,2] · Xiubo Lu[1,2]

Received: 2 January 2020 / Accepted: 14 October 2020 / Published online: 24 January 2021

Abstract

Background LncRNAs play an important role in the regulation of the killing effect of cytotoxic CD8 + T cells in various cancers. However, the role and underlying mechanisms of UCA1 in the killing effect of cytotoxic CD8 + T cells in anaplastic thyroid carcinoma (ATC) are not clear.

Methods UCA1, miR-148a, and PD-L1 expression were detected by quantitative real-time PCR and/or Western blot. The ratio of PD-L1^{+}ATC cells/ATC cells was determined using flow cytometry. The ability of CD8 + T cells to kill target ATC cells was detected by Chromium-51 (^{51}Cr) release assay. The targeted relationship between UCA1 and miR-148a was confirmed by dual-luciferase reporter gene assay.

Results UCA1 and PD-L1 expression levels were elevated in ATC tissues and cells. Silencing UCA1 and PD-L1 enhanced the killing effect of cytotoxic CD8 + T cells on ATC cells. UCA1 negatively regulated the expression of miR-148a, and miR-148a targeted PD-L1 to down-regulate its expression. Besides, we found that UCA1 attenuated the killing effect of cytotoxic CD8 + T cells and reduced cytokine secretion through PD-L1 and miR-148a. Finally, silencing UCA1 or PD-L1 in ATC cells restored the suppression of the killing effect of CD8 + T cells in vivo.

Conclusion UCA1 attenuated the killing effect of cytotoxic CD8 + T cells on ATC cells through the miR-148a/PD-L1 pathway.

Keywords UCA1 · miR-148a · PD-L1 · CD8 + T cells · Anaplastic thyroid carcinoma

Introduction

Anaplastic thyroid carcinoma (ATC) is one of the most aggressive and lethal malignant tumors, with a median survival of fewer than six months, and the effective treatments for ATC are limited [1]. Although ATC only accounts for 1–2% of thyroid carcinoma, it accounts for the majority of thyroid carcinoma-related deaths [1, 2]. Therefore, the effective control and treatment of ATC are of great significance in improving the survival of patients and reducing the mortality of thyroid carcinoma. Studies have shown that tumor cells can avoid the detection by the immune system and inhibit the killing effect of immune cells, such as M1 macrophages, natural killer cells, and cytotoxic CD8 + T cells; thereby, evading elimination [3]. Cytotoxic CD8 + T cells are important immune cells for killing tumor cells, and can directly kill target tumors cells by expressing IFN-γ, TNF-α, perforin, and granzyme B [4, 5]. Therefore, understanding the underlying mechanisms of CD8 + T-cell-mediated killing effect will help in developing a new effective treatment for ATC.

Programmed death-ligand 1 (PD-L1), a type I transmembrane protein, may be expressed on various tumor cells and can contribute to the suppression of antitumor immunity of cytotoxic T cells [6, 7]. PD-1 is primarily expressed on the surface of T cells, which can bind to its ligand PD-L1 and

Electronic supplementary material The online version of this article (https://doi.org/10.1007/s00262-020-02753-y) contains supplementary material, which is available to authorized users.

✉ Xiubo Lu
wxmxn@163.com

1 Thyroid Surgery, The First Affiliated Hospital of Zhengzhou University, No. 1 Jianshe East Rd., Zhengzhou 450052, People's Republic of China

2 Key Laboratory of Thyroid Tumor, The First Affiliated Hospital of Zhengzhou University, Zhengzhou, People's Republic of China

3 Operation Department, The First Affiliated Hospital of Zhengzhou University, Zhengzhou, People's Republic of China

results in the cessation of the T-cell response [8]. Clinical data has shown that the increase of PD-L1 in Glioblastoma promotes the evasion of antitumor effector immune response and predicts worse overall survival [9]. A recent study shows that PD-L1 is highly expressed in ATC tissues, and PD-L1 immune checkpoint blockade has a therapeutic effect on ATC patients [10]. Besides, PD-L1 inhibits the secretion of cytokines and reduces cytotoxicity of lymphocytes via binding to PD-1 on effector CD8 + T cells [11]. The blockade of PD-L1 increases CD8 + T-cell infiltration and cytotoxicity in the ATC mouse model [12]. These findings suggest that PD-L1 inhibits the killing effect of cytotoxic CD8 + T cells in ATC. However, the upstream regulation mechanism of PD-L1 in the killing effect of cytotoxic CD8 + T cells is not clear.

Long noncoding RNAs (lncRNAs) are a kind of RNA transcripts without protein-coding ability [13]. Urothelial carcinoma-associated 1 (UCA1) is an oncogene that is highly expressed in various cancers, such as hypopharyngeal carcinoma, breast cancer, and gastric cancer [14–16]. Besides, UCA1 facilitates epithelial–mesenchymal transition (EMT) and tumor metastasis in breast cancer, glioma, and gastric cancer [15, 17, 18], indicating that UCA1 plays roles in tumor metastasis. Moreover, UCA1 promotes immune escape of gastric cancer cells and predicts poor prognosis in patients with gastric cancer, and the knockout of UCA1 improves the cytotoxicity of cytokine-induced killer cells through regulating PD-L1 [19]. A recent study has reported that UCA1 is up-regulated in ATC tissues and cells, which acts as an oncogene and promotes ATC cell proliferation [20]. However, the role and underlying mechanism of UCA1 in the killing effect of cytotoxic CD8 + T cells in ATC is still not clear.

In this study, UCA1 was up-regulated in ATC tissues and cells, and the overexpression of UCA1 attenuated the cytotoxic CD8 + T-cell killing effect on ATC cells and reduced cytokine secretion through the miRNA/PD-L1 pathway. Moreover, silencing UCA1 or PD-L1 restored the suppression of the killing effect of CD8 + T cells in vivo.

Materials and methods

Sample collection

Thyroid carcinoma tissues and adjacent normal tissues were obtained after resection of thyroid carcinomas from patients at the First Affiliated Hospital of Zhengzhou University. ATC samples were confirmed by the history of thyroid carcinoma, imaging examination, and postoperative pathological diagnosis. Therefore, 10 ATC samples were confirmed and 10 adjacent normal tissues were used as controls. The basic information and treatment of patients are shown in Table 1. All tissues were frozen in liquid nitrogen and stored at – 80 °C. No patients received preoperative chemotherapy. All patients signed informed consent, and this study was approved by the Ethics Committee of the First Affiliated Hospital of Zhengzhou University.

Cell culture and transfection

Human ATC cells (8505C and Hth74) were cultured in Dulbecco's Modified Eagle Medium (DMEM; Gibco, USA) with the addition of 10% fetal bovine serum (FBS; Gibco), 1% Penicillin–Streptomycin (Gibco), 110 mg/l sodium pyruvate, 4500 mg/l D-glucose, and 2 mmol/l L-glutamine, and placed in a 5% CO_2 atmosphere at 37 °C. Human thyroid follicular cells (Nthy-ori 3-1) were cultured in RPMI 1640 medium with the addition of 10% FBS (Gibco) and 1% Penicillin–Streptomycin (Gibco).

Small interference RNAs targeting UCA1 and PD-L1, UCA1-overexpressing, miR-148a mimic, and corresponding control oligonucleotides were cloned into pLVX vectors by Genechem (Shanghai, China). ATC cells were seeded in 12-well plates at a density of 1×10^5 cells/ml and transfected with silencing UCA1 lentivirus (pLV-si-UCA1), silencing PD-L1 lentivirus (pLV-si-PD-L1), UCA1 overexpressing lentivirus (pLV-UCA1), or negative control lentivirus (pLV-ctrl, pLV-si-ctrl).

Quantitative real-time PCR

Total RNAs from ATC tissues (humans and mice), and ATC cells were separated using TRIzol reagent (Invitrogen, USA), and reverse-transcription was performed using High Capacity cDNA Reverse Transcription Kit (Applied Biosystems, USA). Then, cDNA was amplified using SuperScript III Platinum SYBR Green One-Step qRT-PCR Kit (Invitrogen) in an Applied Biosystems 7500 Fast Real-Time PCR System according to the manufacturer's instructions. The relative expressions of UCA1, PD-L1, and miR-148a were measured by the $2^{-\Delta\Delta CT}$ method. GAPDH was used as an internal reference for UCA1 and PD-L1, and U6 was used as an internal reference for miR-148a.

Table 1 The basic information and treatment of patients

Characteristic	ATC ($n = 10$)
Age at initial diagnosis	60.8 ± 8.95
Male, *n* (%)	3 (30%)
Distance metastasis, *n* (%)	8 (80%)
Final disease status, *n* (%)	
AWD	4 (40%)
DOD	6 (60%)
Radiotherapy, *n* (%)	7 (70%)

Western blot analysis

Total proteins were extracted from ATC tissues (humans and mice), and ATC cells using RIPA Lysis and Extraction Buffer (Thermo Scientific, USA) with protease and phosphatase inhibitor cocktails (Thermo Scientific). After the detection of protein concentrations, proteins were subjected to SDS-PAGE, and then transferred to PVDF membranes, and incubated with the primary antibodies overnight at 4 °C. The primary antibodies were used as follows: anti-PD-L1 (1:1000; Cell Signaling Technology, USA), anti-CD8 (1:1000; Abcam, USA), anti-β-actin (1:1000; Cell Signaling Technology). Then, the membranes were incubated with HRP-labeled secondary antibodies (goat anti-rabbit IgG-HRP or goat anti-mouse IgG-HRP) at 25 °C for about 1.5 h. After washing for three times, the bands were visualized using ECL Chemiluminescent Substrate Reagent Kit (Invitrogen).

Isolation of CD8 + T cells

Human peripheral blood was obtained from healthy volunteers, and human peripheral blood mononuclear cells (PBMCs) were isolated using Histopaque-1077 (Sigma-Aldrich, USA). Human CD8 + T cells were isolated using MagniSort Human CD8 Positive Selection Kit (Invitrogen). CD8 + T cells were re-suspended in PBS (1×10^6 cells), and incubated with 25 µl Human T-Activator CD3/CD28 T-cell stimulator (for activating and expanding CD8 + T cells) and 20 U/ml IL-2 (for maintaining the proliferation of CD8 + T cells) at 37 °C for 48 h.

Chromium-51 (^{51}Cr) release assay

The ability of CD8 + T cells to kill target tumor cells was detected by Chromium-51 (^{51}Cr) release assay. Hth74 cells and 8505C cells (1×10^5 cells/ml) were labeled with 100 µCi ^{51}Cr. Then, CD8 + T cells (effector cells) were co-cultured with ^{51}Cr-labeled Hth74 cells or 8505C cells (target cells) at an E: T ratio of 3: 1 and incubated at 37 °C for 4 h. Chromium release from the lysed target cells was determined in the supernatant using a liquid scintillation counter. The percentage of specific lysis was calculated using the following formula: [(experimental counts/minute-spontaneous counts/minute)/(total counts/minute-spontaneous counts/minute)] × 100.

Enzyme-linked immunosorbent assay (ELISA)

Granzyme, TNF-α, and IFN-γ levels in the supernatant of CD8 + T cells were detected by Granzyme Human ELISA Kit (Invitrogen), TNF alpha Human ELISA Kit (Invitrogen), and IFN gamma Human ELISA Kit (Invitrogen).

Dual-luciferase reporter gene assay

293T cells (ATCC) were seeded in 96-well plates and incubated for nearly 24 h. pGL3 luciferase reporter gene vector (Progema, USA) loaded with PD-L1 wild-type (WT) or PD-L1 mutant (Mut) were co-transfected with pre-negative control (NC), miR-148a mimic, pLV-UCA1 + miR-148a mimic into 293T cells using Lipofectamine 2000 (Invitrogen). pGL3 luciferase reporter gene vector loaded with UCA1-WT or UCA1-Mut were co-transfected with pre-NC, miR-148a mimic, NC, miR-148a inhibitor into 293T cells by Lipofectamine 2000. After 48 h, luciferase activity was tested using the Dual-luciferase reporter assay system (Progema).

RNA immunoprecipitation (RIP)

Magna RIP RNA-Binding Protein Immunoprecipitation Kit (Millipore, USA) was used to detect the interaction between UCA1 and miR-148a. Hth74 cells were collected and lysed using RIP lysis buffer. The cell lysate was then incubated with anti-Argonaute2 (anti-Ago2) or normal rabbit IgG as the immunoprecipitating antibody overnight at 4 °C. Purified RNA was quantified by qRT-PCR.

RNA pull-down

According to the reagent manufacturer's instructions, the Pierce Magnetic RNA Protein Pulldown Kit (Thermo Fisher Scientific, USA) was used to perform RNA pull-down experiments to further verify the interaction between UCA1 and miR-148a. Briefly, the cell lysate was mixed with biotinylated UCA1 and incubated with streptavidin agarose magnetic beads (Life Technologies, USA) at 4 °C. The RNA–protein complex was eluted with biotin elution buffer, and the expressions of UCA1 and miR-148a were measured by qRT-PCR.

Flow cytometry

Nthy-ori 3-1 cells (Otwo Biotech (Shenzhen) Inc, HTX1902), Hth74 cells (Otwo Biotech (Shenzhen) Inc, HTX2913), or 8505C cells (Otwo Biotech (Shenzhen) Inc, HTX2543) were re-suspended in phosphate-buffered saline (PBS) containing 1% FBS and 2 mM EDTA and stained with fluorescently conjugated anti-human PD-L1 (Invitrogen) for cell surface staining. Mouse CD8 + T cells were immunostained with fluorescently conjugated anti-CD8 (Invitrogen) for cell surface staining and anti-IFN-γ (Cell

Signaling Technology) for intracellular staining. The data of flow cytometry were obtained on the FACSCalibur flow cytometer (BD, USA) and assessed using CellQuest software.

Tumor models

NOD/Shi-*scid*-IL2rγ^{null} (NOG) mice are immunodeficient mice. In this study, the human PBMCs were intraperitoneally injected into the NOG mice to reconstitute the human immune system. pLV-si-ctrl, pLV-si-UCA1, or pLV-si-PD-L1 were transfected into 8505C cells, then mice were subcutaneously inoculated with 8505C-pLV-si-ctrl (2×10^6 cells), 8505C-pLV-si-UCA1 (2×10^6 cells), 8505C-pLV-si-PD-L1 (2×10^6 cells) one week later after PBMC injection, with five mice in each group. Tumor volume in the three groups was detected at days 5, 10, 15, 20, 25, and 30 after the inoculation of 8505C cells. All mice were sacrificed 30 d later, and tumor tissues were collected. 40% of tumor tissues were used for the detection of CD8, PD-L1, and miR-148a expressions, and the rest of the tumor tissues were used for the separation of tumor-infiltrating CD8 + T cells. The animal experiment was approved by the Ethics Committee of the First Affiliated Hospital of Zhengzhou University.

Tumor-infiltrating CD8 + T-cell isolation

Mouse tumor tissues were dissected, mechanically disaggregated, and digested with 400 U/ml collagenase type I (Gibco) at 37 °C for 30 min. Then, tumors were passed through 70-μm filters and mononuclear cells were separated by Percoll density gradient centrifugation. CD8 + T cells were isolated using MagniSort Mouse CD8 Positive Selection Kit (Invitrogen) for detecting the percentage of IFN-γ + CD8 + T cells/CD8 + T cells.

Statistical analysis

SPSS software (Chicago, USA) was performed for statistical analyses. The data were expressed as mean ± standard deviation (SD). The differences between the two groups were analyzed using Student's *t* test, and the differences among multiple groups were analyzed by one-way analysis of variance followed by Bonferroni's multiple comparison test. $P<0.05$ was considered statistically significant.

Results

UCA1 and PD-L1 expressions were elevated in thyroid carcinoma tissues

First, UCA1 and PD-L1 expressions in human thyroid carcinoma tissues and adjacent normal tissues were detected. As shown in Fig. 1a, b, UCA1 and PD-L1 (CD274) expressions were elevated in thyroid carcinoma tissues than that of adjacent normal tissues, and PD-L1 expression was positively correlated with UCA1 (Pearson $r=0.7591$, $P<0.05$) (Fig. 1c). PD-L1 protein level was elevated in thyroid carcinoma tissues than that of adjacent normal tissues (Fig. 1d). We further detected UCA1 expression in a human thyroid cell line (Nthy-ori 3-1) and ATC cell lines (Hth74 and 8505C) and found that UCA1 was elevated in ATC cells than normal thyroid cells (Fig. 1e). Besides, the ratio of PD-L1$^+$Hth74/Hth74 and PD-L1$^+$8505C/8505C was higher than the ratio of PD-L1$^+$Nthy-ori 3–1/Nthy-ori 3-1 (Fig. 1f), indicating that PD-L1 expression was higher in ATC cells than normal thyroid cells.

UCA1 and PD-L1 attenuated cytotoxic CD8 + T-cell killing effect on ATC cells

In ATC cells, UCA1 overexpression (pLV-UCA1) increased the PD-L1 mRNA level, while silencing UCA1 (pLV-si-UCA1) decreased PD-L1 mRNA level, indicating that UCA1 positively regulated PD-L1 mRNA level (Fig. 2a). Then, Chromium 51 (^{51}Cr)-labeled Hth74 cells or 8505C cells were co-cultured with CD8 + T cells, and we found that pLV-UCA1 inhibited cytotoxic CD8 + T-cell killing effect on ATC cells, while pLV-si-UCA1 or silencing (pLV-si-PD-L1) enhanced the cytotoxic CD8 + T-cell killing effect on ATC cells (Fig. 2b). Also, UCA1 positively regulated PD-L1 protein level in Hth74 cells and 8505C cells (Fig. 2c).

UCA1 attenuated the cytotoxic CD8 + T-cell killing effect through PD-L1

Hth74 cells and 8505C cells were transfected with pLV-UCA1 and/or si-PD-L1. Then, ^{51}Cr-labeled Hth74 cells or 8505C cells were co-cultured with CD8 + T cells. As shown in Fig. 3a, b, pLV-UCA1 inhibited the cytotoxic CD8 + T-cell killing effect on ATC cells (Hth74 or 8505C cells), and pLV-UCA1 + si-PD-L1 enhanced the cytotoxic CD8 + T-cell killing effect on ATC cells. Besides, pLV-UCA1 inhibited the secretion of granzyme, IFN-γ, and TNF-α by CD8 + T cells, and pLV-UCA1 + si-PD-L1 raised the secretion of granzyme, IFN-γ, and TNF-α by CD8 + T cells (Fig. 3c–h).

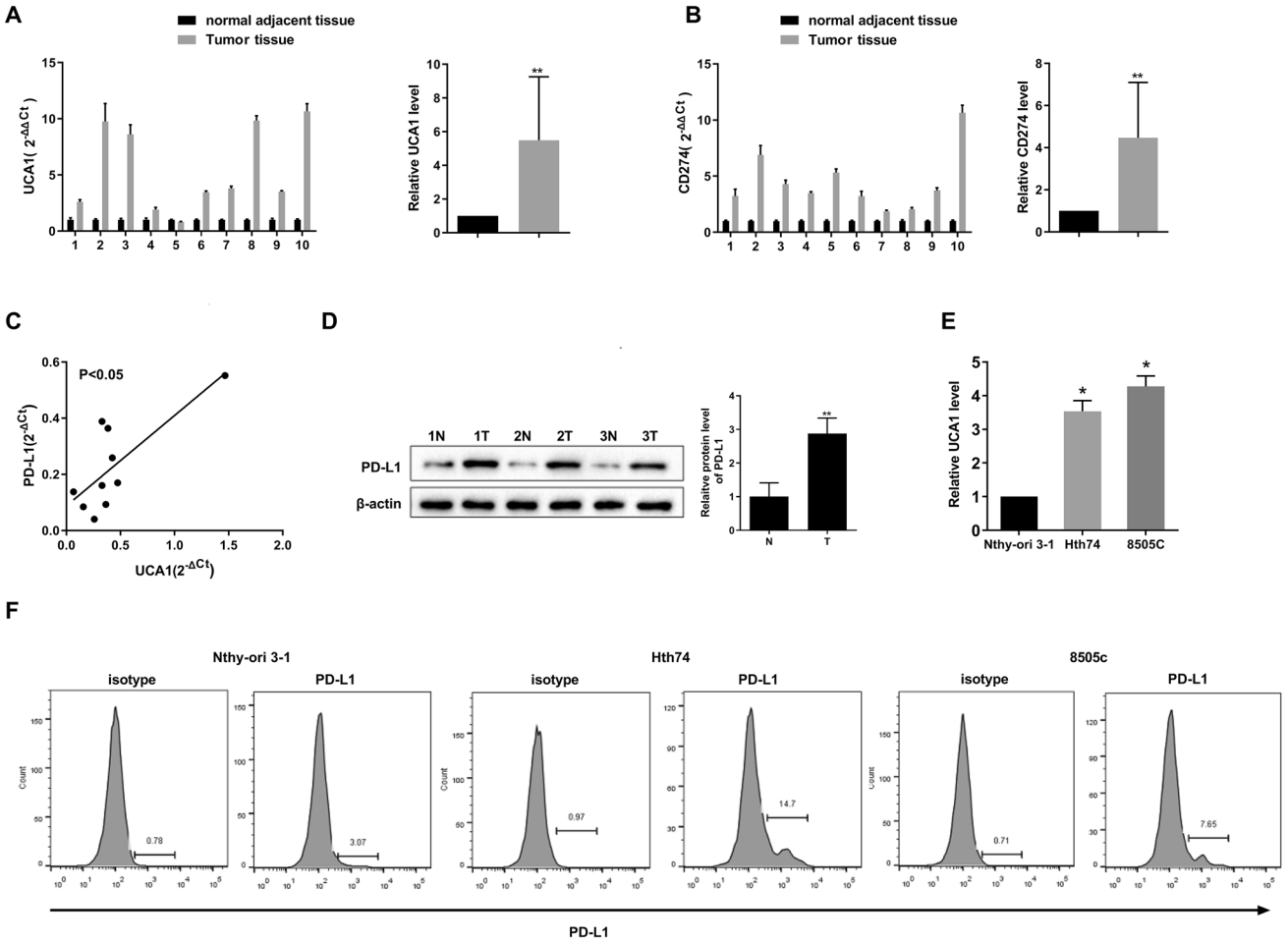

Fig. 1 UCA1 and PD-L1 expressions were elevated in thyroid carcinoma tissues. Thyroid carcinoma tissues ($n=10$) and adjacent normal tissues ($n=10$) were collected. **a** UCA1 expressions in thyroid carcinoma tissues and adjacent normal tissues were detected using quantitative real-time PCR (qRT-PCR). **b** PD-L1 (CD274) mRNA level in thyroid carcinoma tissues and adjacent normal tissues was detected using qRT-PCR. **c** CD274 expression was positively correlated with UCA1 expression. **d** The PD-L1 protein levels in thyroid carcinoma tissues and adjacent normal tissues were detected using Western blot. **e** UCA1 expressions in the human thyroid cell line (Nthy-ori 3-1) and ATC cell lines (Hth74 and 8505C) were detected using qRT-PCR. **f** The ratio of PD-L1$^+$Nthy-ori 3-1/Nthy-ori 3-1 cells, PD-L1$^+$Hth74/Hth74 cells, and PD-L1$^+$8505C/8505C cells were detected by flow cytometry. $^*P < 0.05$ vs. Nthy-ori 3-1. $^{**}P<0.01$ vs. adjacent normal tissues

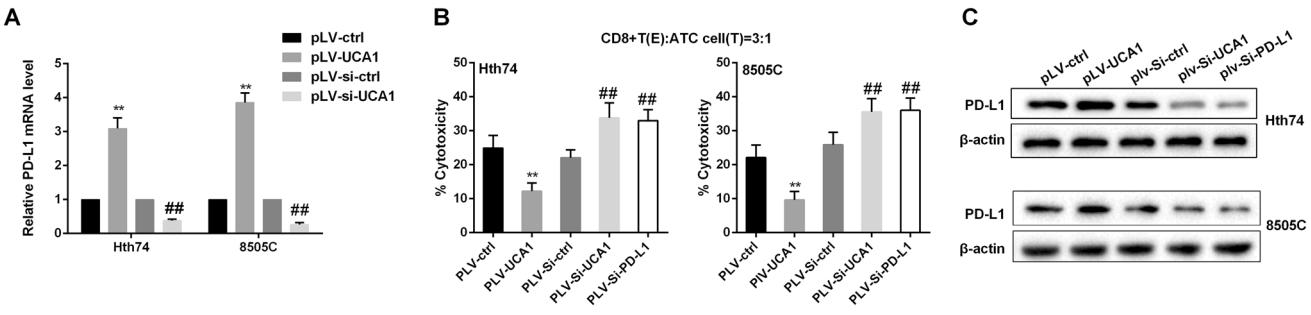

Fig. 2 UCA1 and PD-L1 attenuated the cytotoxic CD8+T-cell killing effect on ATC cells. **a** In ATC cells, UCA1 positively regulated the PD-L1 mRNA level. **b** Chromium 51 (^{51}Cr)-labeled Hth74 cells or 8505C cells were co-cultured with CD8+T cells at an effector (CD8+T cells) to target (^{51}Cr-Hth74 or 8505C cells) ratio (E:T) of 3:1 to detect the cytotoxic CD8+T-cell killing effect on ATC cells. **c** In ATC cells, UCA1 positively regulated the PD-L1 protein level. $^{**}P<0.01$ vs. pLV-ctrl, $^{\#\#}P<0.01$ vs. pLV-si-ctrl. *Ctrl* control

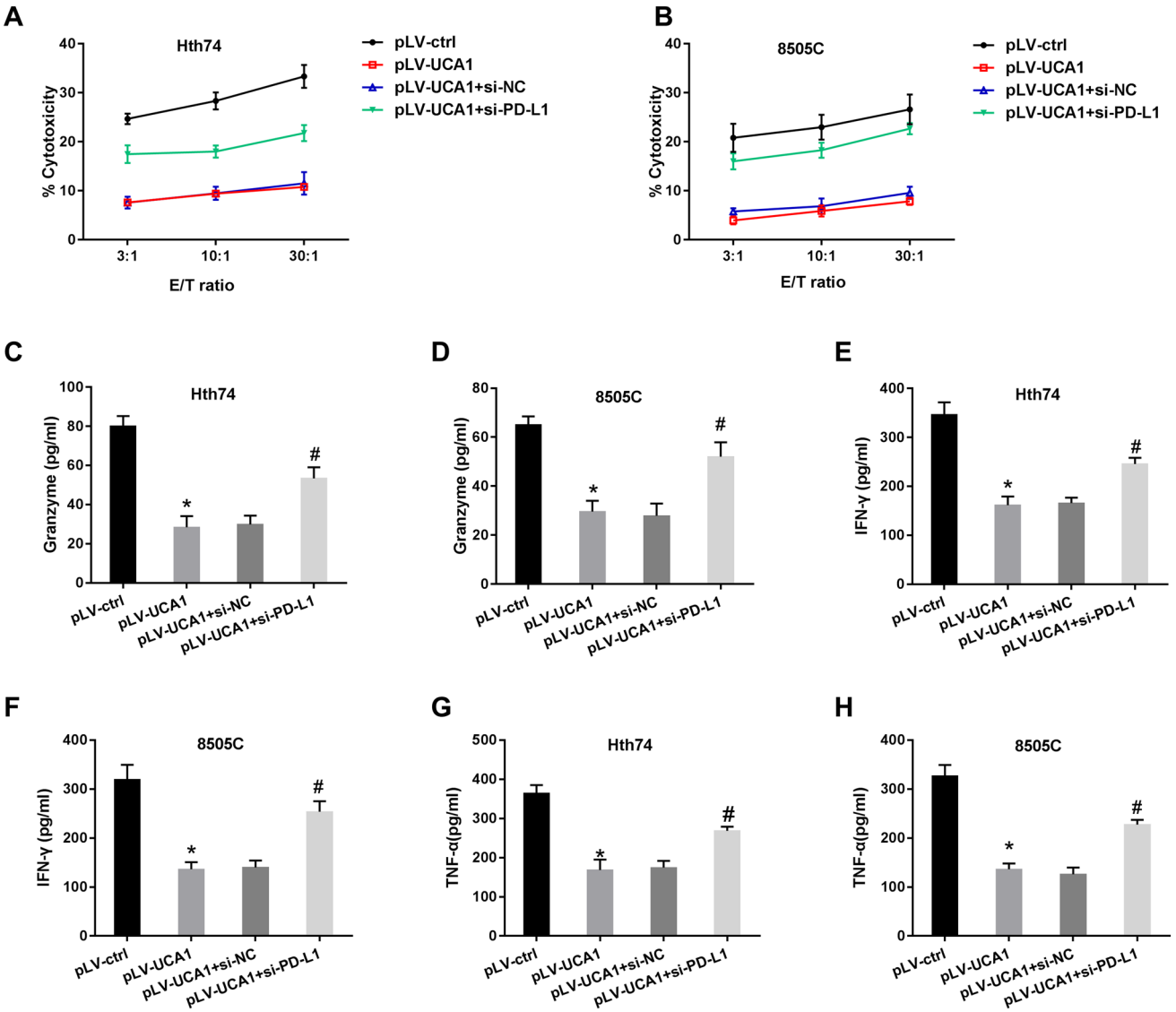

Fig. 3 UCA1 attenuated the cytotoxic CD8 + T-cell killing effect through PD-L1. **a**–**b** ATC cells (Hth74 or 8505C cells) were divided into pLV-ctrl, pLV-UCA1, pLV-UCA1 + si-NC, pLV-UCA1 + si-PD-L1 groups. Then, CD8 + T cells were co-cultured with ATC cells at an E: T ratio of 3:1. The cytotoxic CD8 + T-cell killing effect on ATC cells was detected by ^{51}Cr release assay. **c**–**h** Granzyme, IFN-γ, and TNF-α levels were detected using ELISA. $^{*}P < 0.05$ vs. pLV-ctrl, $^{\#}P < 0.05$ vs. pLV-UCA1 + si-NC. *Ctrl* control, *NC* negative control

UCA1 promoted PD-L1 expression through miR-148a

According to the prediction of bioinformatics software (DIANA), there were binding sites between UCA1 and miR-148a (Fig. 4a). Dual-luciferase reporter gene assay showed that miR-148a mimic reduced the luciferase activity of UCA1 WT, while the miR-148a mimic did not change the luciferase activity of UCA1 Mut (Fig. 4b). On the contrary, the miR-148a inhibitor increased the luciferase activity of UCA1 WT (Fig. 4b), and the overexpression of miR-148a down-regulated the expression of UCA1 (Supplementary Fig. 2a). Besides, miR-148a expression was down-regulated in thyroid carcinoma tissues than adjacent normal tissues (Fig. 4c). Moreover, we found that pLV-UCA1 increased UCA1 expression and decreased miR-148a expression in Hth74 and 8505C cells, pLV-si-UCA1 decreased UCA1 expression and increased miR-148a expression (Fig. 4d, e). RIP assay showed that UCA1 and miR-148a were accumulated in the precipitates using the Ago2 antibody (Fig. 4f). Besides, we used Biotin-labeled UCA1 probes to perform RNA pull down to verify the interaction between UCA1 and miR-148a again (Supplementary Fig. 2b). These findings indicated that UCA1 interacted with miR-148a and negatively regulated miR-148a. Bioinformatics software (miRWalk) also predicted there were binding sites between miR-148a and PD-L1 (Fig. 4g). After transfected pre-NC or

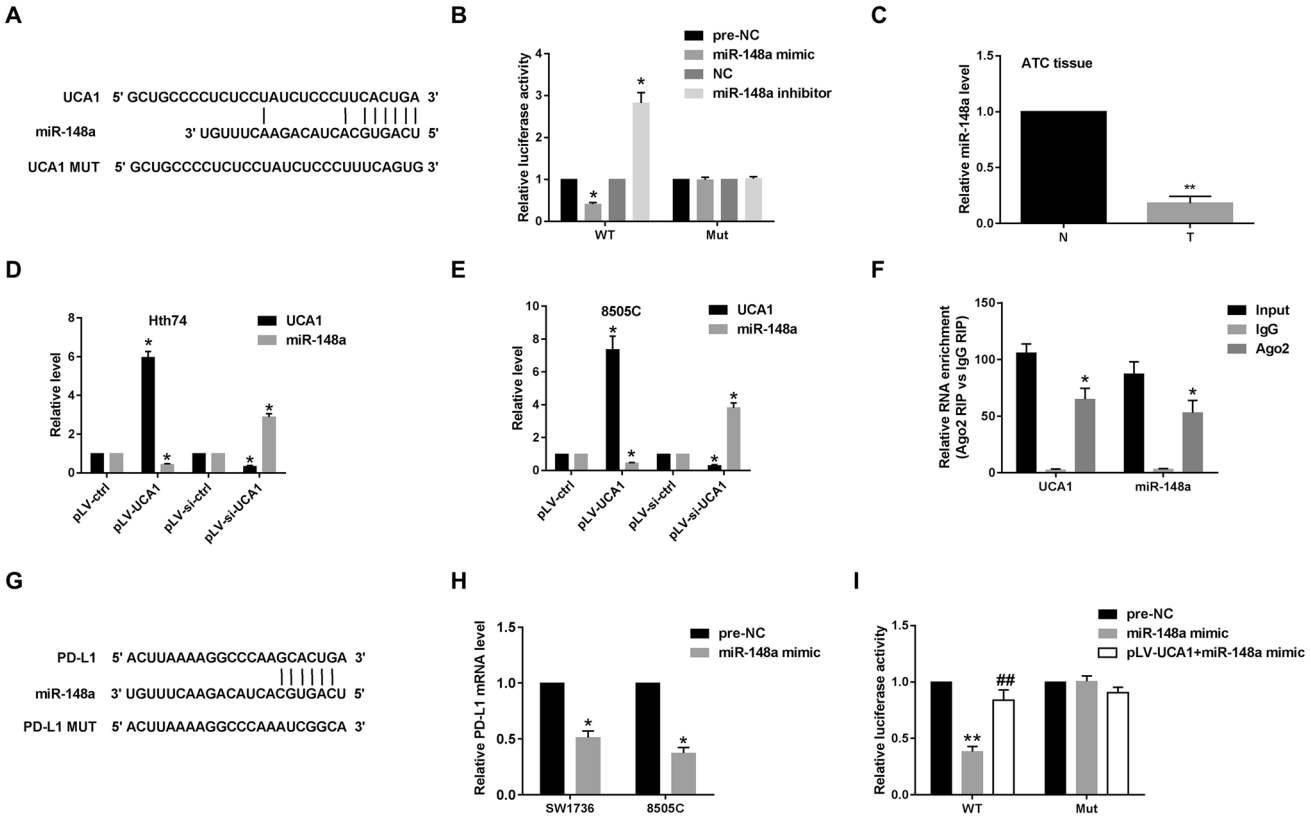

Fig. 4 UCA1 promoted PD-L1 expression through miR-148a. **a** Bioinformatics software (DIANA) predicted that there were binding sites between UCA1 and miR-148a. **b** A dual-luciferase reporter gene assay was performed to measure the targeted relationship between UCA1 and miR-148a in 293T cells. $^{*}P<0.05$ vs. pre-NC or NC. **c** miR-148a expression in thyroid carcinoma tissues and adjacent normal tissues was detected using qRT-PCR. $^{**}P<0.01$ vs. normal tissues. **d**–**e** Hth74 and 8505C cells were divided into pLV-ctrl, pLV-UCA1, pLV-si-ctrl, pLV-si-UCA1 groups. UCA1 and miR-148a expressions were detected using qRT-PCR. $^{*}P<0.05$ vs. pLV-ctrl or pLV-si-ctrl. **f** The interaction between UCA1 and miR-148a was detected by RIP assay, and qRT-PCR was performed to detect UCA1 and miR-148a expressions in the precipitates. $^{*}P<0.05$ vs. IgG. **g** Bioinformatics software predicted that there were binding sites between miR-148a and PD-L1. **h** Hth74 and 8505C cells were transfected with pre-NC or miR-148a mimic. PD-L1 mRNA level was detected by qRT-PCR. $^{*}P<0.05$ vs. pre-NC. **i** miR-148a mimic and/or pLV-UCA1, PD-L1 3′UTR WT, or Mut were co-transfected into 293T cells. Dual-luciferase reporter gene assay was performed to detect the regulation of UCA1/miR-148a in transcriptional activation of PD-L1. $^{**}P<0.01$ vs. pre-NC, $^{\#\#}P<0.01$ vs. miR-148a mimic. *Ctrl* control, *NC* negative control

miR-148a mimic into Hth74 and 8505C cells, we observed miR-148a mimic decreased PD-L1 mRNA level (Fig. 4h). Finally, miR-148a mimic decreased the luciferase activity of PD-L1 3′UTR WT, and the pLV-UCA1 + miR-148a mimic increased the luciferase activity of PD-L1 3′UTR WT (Fig. 4i).

UCA1 attenuated the cytotoxic CD8 + T-cell killing effect and reduced cytokine secretion through miR-148a

To determine whether UCA1 attenuated the cytotoxic CD8 + T-cell killing effect through regulating miR-148a, pLV-UCA1 and miR-148a mimic were transfected into Hth74 and 8505C cells. The ^{51}Cr-labeled Hth74 and 8505C cells were co-cultured with CD8 + T cells. We found that the cytotoxic CD8 + T-cell killing effect on Hth74 and 8505C cells was decreased in the pLV-UCA1 group, while the cytotoxic CD8 + T-cell killing effect on ATC cells was enhanced in the pLV-UCA1 + miR-148a mimic group (Fig. 5a, b). Besides, pLV-UCA1 reduced the levels of granzyme, IFN-γ, and TNF-α secreted by CD8 + T cells, pLV-UCA1 + miR-148a mimic increased the levels of granzyme, IFN-γ, and TNF-α secreted by CD8 + T cells (Fig. 5c–h).

UCA1 and PD-L1 in ATC cells were critical for suppression of the killing effect of CD8 + T cells in vivo

To investigate the antitumor effects by target human T cells, NOG mice were subcutaneously inoculated with 8505C cells transfected with pLV-si-ctrl, pLV-si-UCA1, or pLV-si-PD-L1 one week later after PBMC injection. As shown in Fig. 6a, tumor volume was lessened in the pLV-si-UCA1 and pLV-si-PD-L1 groups than the pLV-si-ctrl

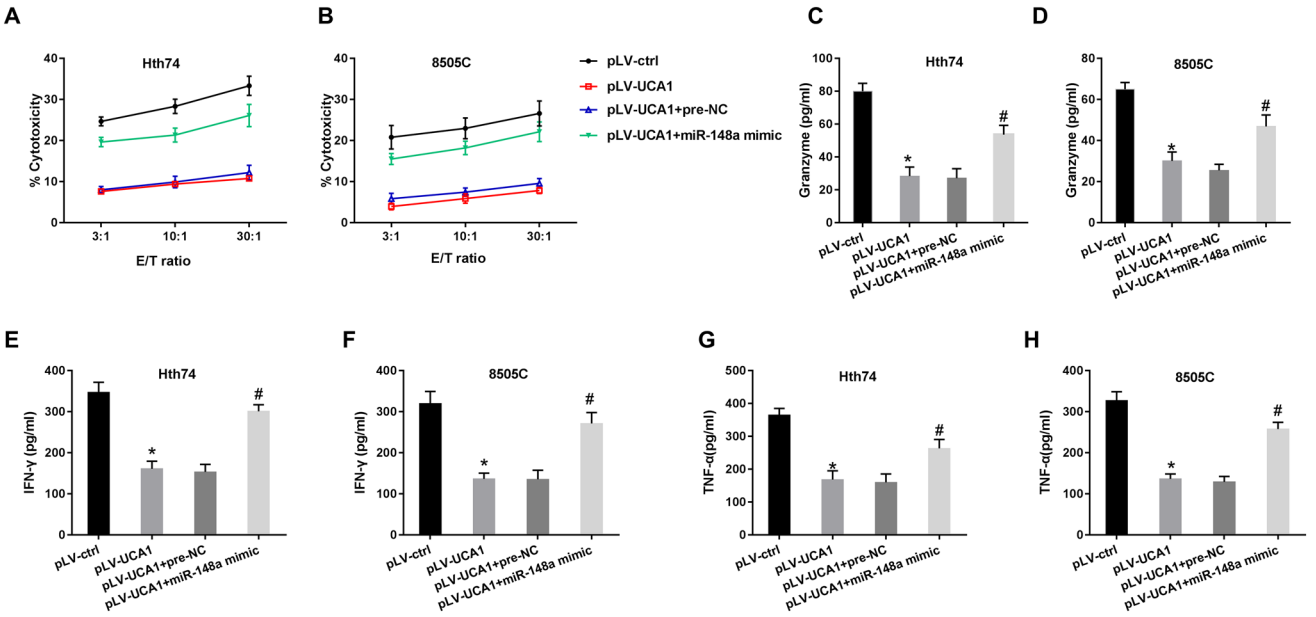

Fig. 5 UCA1 attenuated the cytotoxic CD8 + T-cell killing effect and reduced cytokine secretion through miR-148a. Hth74 and 8505C cells were transfected with pLV-ctrl, pLV-UCA1, pLV-UCA1 + pre-NC, pLV-UCA1 + miR-148a mimic. The ^{51}Cr-labeled Hth74 and 8505C cells were co-cultured with CD8 + T cells. **a**–**b** The cytotoxic CD8 + T-cell killing effect on ATC cells was detected by ^{51}Cr release assay. **c**–**d** Granzyme secreted by CD8 + T cells was detected by ELISA. **e**–**f** IFN-γ secreted by CD8 + T cells was detected by ELISA. **g**–**h** TNF-α secreted by CD8 + T cells was detected by ELISA. $^{*}P < 0.05$ vs. pLV-ctrl, $^{\#}P < 0.05$ vs. pLV-UCA1 + pre-NC. *Ctrl* control, *NC* negative control

group, indicating that UCA1 or PD-L1 suppressed the killing effect of CD8 + T cells. Besides, the percentage of CD8 + IFN-γ + T cells/CD8 + T cells was increased in the pLV-si-UCA1 and pLV-si-PD-L1 groups than the pLV-si-ctrl group (Fig. 6b). Compared with the pLV-si-ctrl group, CD8 protein level was up-regulated in the pLV-si-UCA1 and pLV-si-PD-L1 groups, while the PD-L1 protein level was down-regulated in the pLV-si-UCA1 and pLV-si-PD-L1 groups (Fig. 6c). miR-148a expression was increased in the pLV-si-UCA1 group than the pLV-si-ctrl group, while pLV-si-PD-L1 did not affect its expression (Fig. 6d), indicating that miR-148a was negatively regulated by UCA1 in vivo.

Discussion

LncRNAs have been identified to act as oncogenes or tumor suppressor genes in a variety of cancers [21–23]. Besides, plenty of LncRNAs are involved in the suppression of the killing effect of cytotoxic T cells [24, 25]. However, studies focused on LncRNAs in regulating the killing effect of cytotoxic T cells in ATC are lacked. In this study, we found that UCA1 was up-regulated in ATC tissues and cells, and silencing UCA1 reduced tumor volume, indicating that UCA1 acted as an oncogene in ATC. Besides, UCA1 overexpression reduced the killing effect of cytotoxic CD8 + T cells on ATC cells, and silencing UCA1 promoted the killing effect of cytotoxic CD8 + T cells on ATC cells. Therefore, this study revealed that UCA1 played an important role in attenuating the killing effect of cytotoxic CD8 + T cells on ATC cells, which will be helpful to guide the treatment of ATC.

Several studies have shown that immune-related miRNAs can be sponged by LncRNAs to regulate the killing effect of cytotoxic T cells on cancers [19, 26]. miR-148a is one of these immune-related miRNAs and exerts its functional role in the regulation of T cell-induced cytotoxicity in cancers [27]. Besides, miR-148a exerts a tumor-suppressive role in many cancers and usually is down-regulated in tumor tissues and cells, including in papillary thyroid carcinomas [28, 29]. However, whether miR-148a regulates the killing effect of cytotoxic CD8 + T cells on ATC cells is largely unknown. In this study, we found that miR-148a was remarkably down-regulated in ATC tissues. 293T cells co-transfected with miR-148a mimic and UCA1-WT exhibited a significant decrease in the luciferase activity, whereas the co-transfection of miR-148a mimic and UCA1-Mut had little influence on the luciferase activity, which confirmed the target relationship between UCA1 and miR-148a. After the overexpression of UCA1 in ATC cells (Hth74 and 8505C cells), miR-148a was down-regulated, and the UCA1 knockdown obtained an opposite result. To investigate the in-depth underlying mechanism of UCA1/miR-148a, pLV-UCA1 or pLV-UCA1 + miR-148a mimic were transfected into ATC

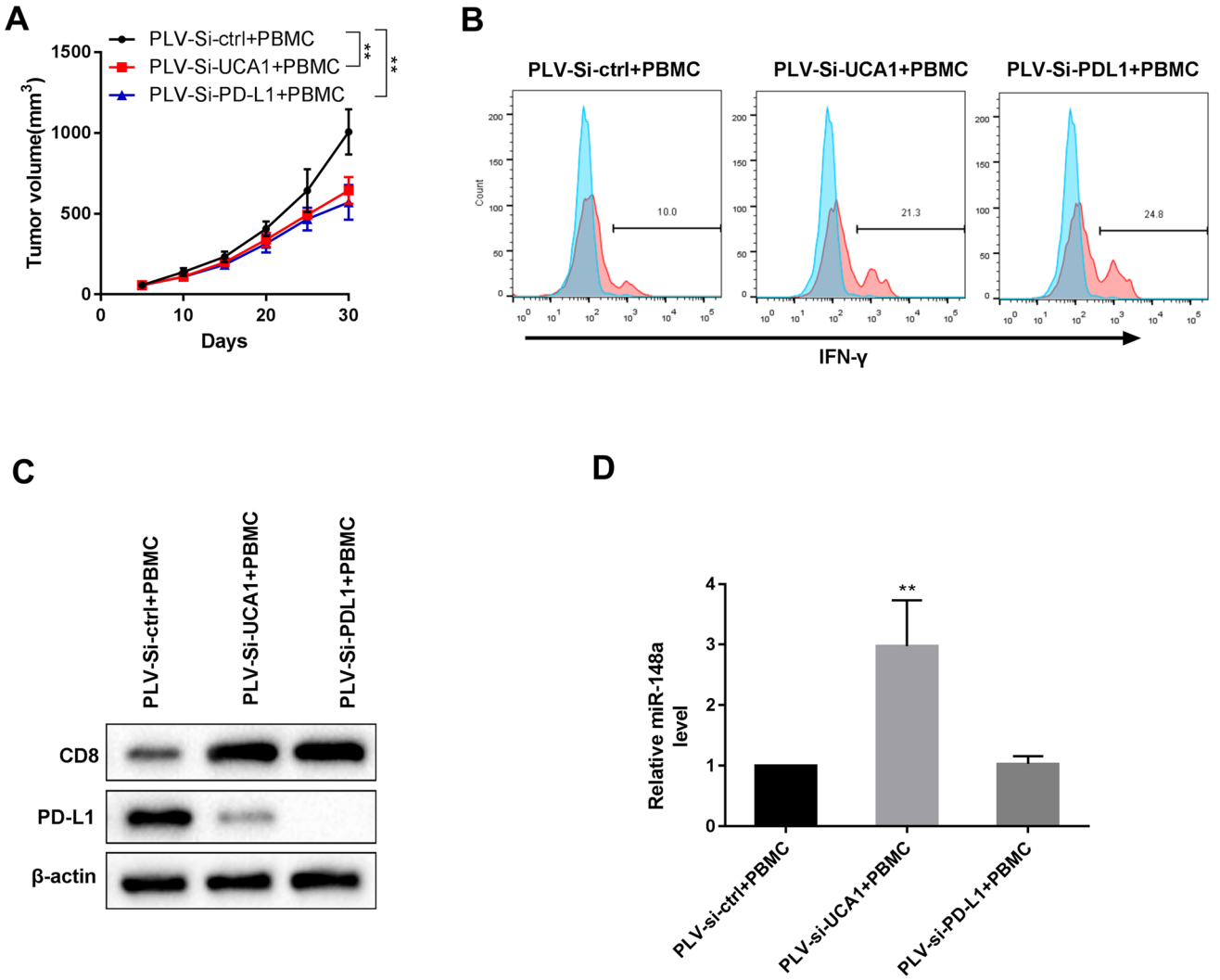

Fig. 6 UCA1 and PD-L1 in ATC cells were critical for suppression of the killing effect of CD8 + T cells in vivo. NOD/Shi-*scid*-IL2rγ^{null} (NOG) mice were divided into pLV-si-ctrl + PBMC, pLV-si-UCA1 + PBMC, pLV-si-PD-L1 + PBMC groups, with five mice in each group. **a** Tumor volume in the three groups was detected at days 5, 10, 15, 20, 25, 30. **b** The percentage of CD8 + IFN-γ + T cells in the three groups was detected by flow cytometry. **c** CD8, PD-L1, and miR-148a expressions in these three groups. *Ctrl* control, *NC* negative control. $^{**}P < 0.01$ vs. pLV-si-ctrl + PBMC

cells, and the results showed that pLV-UCA1 decreased the killing effect of cytotoxic CD8 + T cells on ATC cells, and miR-148a mimic abolished the inhibition effect of UCA1 overexpression. Therefore, our study first demonstrated the role of UCA1/miR-148a in regulating the killing effect of cytotoxic CD8 + T cells on ATC cells.

PD-L1 is an important molecule that involved in immune escape and is overexpressed in many tumor cells and has shown efficacy in suppressing immune response in many cancers, such as pancreatic cancer, bladder cancer, and ATC, and PD-L1 is highly expressed in ATC tumor tissues, which is a predictor for progression-free survival and overall survival of ATC patients [30–33]. PD-1/PD-L1 blockade can enhance the function of cytotoxic T cells, which helps kill the cancer cells and eliminate the tumor [34, 35]. However, the role and mechanism of PD-L1 in the killing effect of CD8 + T cells in ATC are not fully understood. Here, we discovered that PD-L1 was up-regulated in ATC tissues and cells, and silencing PD-L1 enhanced the killing effect of CD8 + T cells on ATC cells, and increased the secretion of granzyme, TNF-α, and IFN-γ by CD8 + T cells. Besides, our results showed that the expression of UCA1 was positively correlated with the mRNA level of PD-L1 (Fig. 1) and PD-L1 mediated the changes in CD8 + T-cell toxicity induced by UCA1 (Fig. 3). Therefore, we further explored the potential mechanism of UCA1 regulating PD-L1. Multiple previous studies have shown that PD-L1 can be the target of cancer-related miRNAs in many cancers [36, 37]. Here, through the analysis of

bioinformatics online software, we found that miR-148a was a potential regulatory miRNA of PD-L1 transcription, and further experiments confirmed that the PD-L1 mRNA level was negatively regulated by miR-148a. Combined with our previous findings that UCA1 targeted miR-148a, and UCA1 reversed the inhibition effect of miR-148a mimic on the luciferase activity of PD-L1 3′UTR, indicating the regulation role of UCA1/miR-148a in PD-L1 expression.

In conclusion, UCA1 was found to be up-regulated in ATC tissues and cells and targeted miR-148a. The overexpression of UCA1 attenuated the killing effect of cytotoxic CD8 + T cell on ATC cells and reduced cytokine secretion through the miR-148a/PD-L1 pathway in vitro. Silencing UCA1 or PD-L1 restored the suppression of the killing effect of CD8 + T cells in vivo. The flow chart of the pathway mechanism is shown in Supplementary Fig. 1.

Author contribution XW designed this experiment and performed the experiments. XW and YZ edited this manuscript. YZ and JZ collected data and performed the statistical analysis. JZ, CY and MT revised this manuscript. XL made substantial contributions to the conception, design, and critical revision of the manuscript. All authors read and approved the final manuscript.

Funding None.

Compliance with ethical standards

Conflict of interest The authors have no actual or potential conflicts of interest to declare.

Ethical approval The study was approved by the ethics committee of The First Affiliated Hospital of Zhengzhou University.

References

1. Molinaro E et al (2017) Anaplastic thyroid carcinoma: from clinicopathology to genetics and advanced therapies. Nat Rev Endocrinol 13:644
2. Cao X et al (2019) Targeting super-enhancer-driven oncogenic transcription by CDK7 inhibition in anaplastic thyroid carcinoma. Thyroid 29(6):809–823
3. Hanahan D, Weinberg RA (2011) Hallmarks of cancer: the next generation. Cell 144(5):646–674
4. Andrada E, Liébana R, Merida I (2017) Diacylglycerol kinase ζ limits cytokine-dependent expansion of CD8(+) T cells with broad antitumor capacity. EBioMedicine 19:39–48
5. Hodge G et al (2014) Lung cancer is associated with decreased expression of perforin, granzyme B and interferon (IFN)-γ by infiltrating lung tissue T cells, natural killer (NK) T-like and NK cells. Clin Exp Immunol 178(1):79–85
6. Goodman A, Patel SP, Kurzrock R (2017) PD-1-PD-L1 immune-checkpoint blockade in B-cell lymphomas. Nat Rev Clin Oncol 14(4):203–220
7. Frydenlund N, Mahalingam M (2017) PD-L1 and immune escape: insights from melanoma and other lineage-unrelated malignancies. Hum Pathol 66:13–33
8. Pardoll DM (2012) The blockade of immune checkpoints in cancer immunotherapy. Nat Rev Cancer 12(4):252–264
9. Han J, Hong Y, Lee YS (2017) PD-L1 expression and combined status of PD-L1/PD-1-positive tumor infiltrating mononuclear cell density predict prognosis in glioblastoma patients. J Pathol Transl Med 51(1):40–48
10. Bastman JJ et al (2016) Tumor-infiltrating T Cells and the PD-1 checkpoint pathway in advanced differentiated and anaplastic thyroid cancer. J Clin Endocrinol Metab 101(7):2863–2873
11. Lau J et al (2017) Tumour and host cell PD-L1 is required to mediate suppression of anti-tumour immunity in mice. Nat Commun 8:14572–14572
12. Brauner E et al (2016) Combining BRAF inhibitor and anti PD-L1 antibody dramatically improves tumor regression and anti tumor immunity in an immunocompetent murine model of anaplastic thyroid cancer. Oncotarget 7(13):17194–17211
13. Dong P et al (2019) Long noncoding RNA NEAT1 drives aggressive endometrial cancer progression via miR-361-regulated networks involving STAT3 and tumor microenvironment-related genes. J Exp Clin Cancer Res 38(1):295
14. Qian Y et al (2017) Upregulation of the long noncoding RNA UCA1 affects the proliferation, invasion, and survival of hypopharyngeal carcinoma. Mol Cancer 16(1):68
15. Li GY et al (2018) Long non-coding RNAs AC026904.1 and UCA1: a "one-two punch" for TGF-beta-induced SNAI2 activation and epithelial-mesenchymal transition in breast cancer. Theranostics 8(10):2846–2861
16. Yang Z et al (2018) Long non-coding RNA UCA1 upregulation promotes the migration of hypoxia-resistant gastric cancer cells through the miR-7-5p/EGFR axis. Exp Cell Res 368(2):194–201
17. He Z et al (2017) The lncRNA UCA1 interacts with miR-182 to modulate glioma proliferation and migration by targeting iASPP. Arch Biochem Biophys 623–624:1–8
18. Zuo ZK et al (2017) TGFbeta1-induced LncRNA UCA1 upregulation promotes gastric cancer invasion and migration. DNA Cell Biol 36(2):159–167
19. Wang CJ et al (2019) The lncRNA UCA1 promotes proliferation, migration, immune escape and inhibits apoptosis in gastric cancer by sponging anti-tumor miRNAs. Mol Cancer 18(1):115
20. Wang Y, Hou Z, Li D (2018) Long noncoding RNA UCA1 promotes anaplastic thyroid cancer cell proliferation via miR135a-mediated cmyc activation. Mol Med Rep 18(3):3068–3076
21. Shi D et al (2019) LncRNA AFAP1-AS1 promotes tumorigenesis and epithelial-mesenchymal transition of osteosarcoma through RhoC/ROCK1/p38MAPK/Twist1 signaling pathway. J Exp Clin Cancer Res 38(1):375
22. Zeng Z et al (2019) LncRNA-MTA2TR functions as a promoter in pancreatic cancer via driving deacetylation-dependent accumulation of HIF-1α. Theranostics 9(18):5298–5314
23. Li P et al (2019) ZNNT1 long noncoding RNA induces autophagy to inhibit tumorigenesis of uveal melanoma by regulating key autophagy gene expression. Autophagy 16(7):1186–1199
24. Yu Z et al (2019) Long non-coding RNA FENDRR acts as a miR-423-5p sponge to suppress the Treg-mediated immune escape of hepatocellular carcinoma cells. Mol Ther Nucleic Acids 17:516–529
25. Hu Q et al (2019) Oncogenic lncRNA downregulates cancer cell antigen presentation and intrinsic tumor suppression. Nat Immunol 20(7):835–851
26. Yan K et al (2019) Repression of lncRNA NEAT1 enhances the antitumor activity of CD8(+)T cells against hepatocellular carcinoma via regulating miR-155/Tim-3. Int J Biochem Cell Biol 110:1–8
27. Mari L et al (2018) microRNA 125a regulates MHC-I expression on esophageal adenocarcinoma cells, associated with suppression

of antitumor immune response and poor outcomes of patients. Gastroenterology 155(3):784–798
28. Friedrich M et al (2017) The role of the miR-148/-152 family in physiology and disease. Eur J Immunol 47(12):2026–2038
29. Han C et al (2017) Downregulation of cyclin-dependent kinase 8 by microRNA-148a suppresses proliferation and invasiveness of papillary thyroid carcinomas. Am J Cancer Res 7(10):2081–2090
30. Feng M et al (2017) PD-1/PD-L1 and immunotherapy for pancreatic cancer. Cancer Lett 407:57–65
31. Inman BA et al (2017) Atezolizumab: A PD-L1-blocking antibody for bladder cancer. Clin Cancer Res 23(8):1886–1890
32. Ahn S et al (2017) Comprehensive screening for PD-L1 expression in thyroid cancer. Endocr Relat Cancer 24(2):97–106
33. Cantara S et al (2019) Blockade of the programmed death ligand 1 (PD-L1) as potential therapy for anaplastic thyroid cancer. Endocrine 64(1):122–129
34. Osada T et al (2015) CEA/CD3-bispecific T cell-engaging (BiTE) antibody-mediated T lymphocyte cytotoxicity maximized by inhibition of both PD1 and PD-L1. Cancer Immunol Immunother 64(6):677–688
35. Martínez-Lostao L, Anel A, Pardo J (2015) How do cytotoxic lymphocytes kill cancer cells? Clin Cancer Res 21(22):5047–5056
36. Gao L et al (2019) MiR-873/PD-L1 axis regulates the stemness of breast cancer cells. EBioMedicine 41:395–407
37. Chen Y et al (2019) LIN28/let-7/PD-L1 pathway as a target for cancer immunotherapy. Cancer Immunol Res 7(3):487–497